NASA TM-81188

NASA Technical Memorandum 81788

NASA-TM-81788 19800011746

TRANSONIC UNSTEADY AIRLOADS ON AN ENERGY EFFICIENT TRANSPORT WING WITH OSCILLATING CONTROL SURFACES

M. C. SANDFORD, R. H. RICKETTS,
F. W. CAZIER, JR., AND H. J. CUNNINGHAM

MARCH 1980

National Aeronautics and
Space Administration

Langley Research Center
Hampton, Virginia 23665

TRANSONIC UNSTEADY AIRLOADS ON AN ENERGY EFFICIENT TRANSPORT WING WITH OSCILLATING CONTROL SURFACES

M. C. Sandford,* R. H. Ricketts,** F. W. Cazier, Jr.,* and H. J. Cunningham*
NASA Langley Research Center
Hampton, VA 23665

Abstract

An aspect-ratio 10.8 supercritical wing with oscillating control surfaces is described. The wing is instrumented with 252 static orifices and 164 in situ dynamic pressure transducers for studying the effects of control surface deflection on steady and unsteady pressures at transonic speeds. Selected results from initial wind-tunnel tests conducted in the Langley Transonic Dynamics Tunnel are discussed. Unsteady pressure results are presented for two trailing-edge control surfaces oscillating separately at the design Mach number of 0.78. Some experimental results are compared with analytical results obtained by using linear lifting-surface theory.

Symbols

b	wing root semichord, 0.400 m
c	wing local chord, m
C_L	wing lift coefficient
f	frequency of oscillating control surface, Hertz
k	reduced frequency ratio, $\frac{b\omega}{V}$
M	free-stream Mach number
RN	Reynolds number based on wing average chord of 0.425 m
V	free-stream velocity, m/s
t/c	local thickness-to-chord ratio
x/c	fraction-of-chord
α	wing angle of attack, degrees, positive leading edge up
δ	control surface deflection angle, degrees, positive trailing edge down
ΔC_p	unsteady lifting pressure coefficient
η	fraction of semispan
ω	circular frequency of oscillating control surface, radians/s

Introduction

Currently there is considerable interest in applying active control techniques to new and derivative airplane designs. This is particularly true for configurations, such as energy efficient transport, that operate at transonic speeds. Although considerable effort is being placed on developing methods for predicting unsteady transonic aerodynamics, and significant progress has been made[1,2] no theoretical method has been developed to the point that it can be used to predict unsteady transonic loads reliably. Therefore, a research program employing a large three-dimensional wing model was initiated at the NASA Langley Research Center to investigate the effects of oscillating control surfaces on transonic unsteady aerodynamics. The primary objective of this research program is to generate a comprehensive data base of measured unsteady pressures. This data base will be used in the design of active control systems for proposed energy efficient transport configurations and in validating transonic unsteady aerodynamic theories currently being formulated.

The supercritical wing configuration is equipped with 10 oscillating control surfaces. The wing is extensively instrumented to measure both steady and unsteady pressures. Initial wind-tunnel tests have been conducted in the Langley Transonic Dynamics Tunnel at Mach numbers up to 0.82. Model parameters investigated include wing angle of attack, control surface static deflection angles, and control surface oscillating deflections and frequencies.

The purpose of this paper is to present selected results from these initial tests in which two trailing-edge control surfaces were oscillated to generate unsteady aerodynamic pressures. Although the focus is on measured unsteady data, analytical results obtained using subsonic lifting-surface theory[3] are compared with measured results.

Wind Tunnel Model

General

The model consisted of a half-body fuselage similar to that of a "wide-body" transport and a stiff semispan wing having a planform representative of current energy efficient transport designs. The model was mounted on the tunnel sidewall on a turntable mechanism which allowed the angle of attack to be varied (see figure 1).

Geometry

A sketch of the wing is presented in figure 2. The wing has a leading-edge sweepback angle of 28.8°, an aspect-ratio of 10.76, and a semispan of 2.286 meters. The side of the half-body fuselage was located at a wing station 0.219 m.

The wing is equipped with 10 oscillating control surfaces. Outlined in figure 2 are five leading-edge control surfaces hinged about the 15-percent chord and five trailing-edge control surfaces hinged about the 80-percent chord. For

*Aero-Space Technologist, Structures and Dynamics Div.

**Aero-Space Technologist, Structures and Dynamics Div.

these initial wind-tunnel tests only two trailing-edge control surfaces, shown in figure 2 by the cross-hatched areas, were oscillated to generate unsteady airloads. These two control surfaces are designated hereafter as the inboard control surface and the outboard control surface.

The wing contour was formed from three different supercritical airfoils. These three airfoils were located at wing stations 0.219 m, 0.876 m and 2.286 m and had thickness-to-chord ratios of 0.16, 0.14, and 0.12, respectively. The three supercritical airfoil shapes are shown in figure 3. Straight line interpolation along constant percent chords was used between adjacent airfoil sections. The section twist angles at each station, referenced to a horizontal reference plane, are also shown in figure 3.

Construction

The wing was constructed from aluminum alloy and consisted of upper and lower sections. Each section was stiffened in bending by a boron filament insert bonded to the internal cutout area shown in figure 4. The sections were permanently bonded together to form a box cross section. This type of construction produced a stiff, lightweight wing structure whose fundamental frequency (23 Hz) was well above the maximum control surface excitation frequency used during the tests (15 Hz). These requirements for a stiff, high frequency wing structure were dictated by the need to minimize the dynamic and static deformations of the model due to aerodynamic loads.

Lightweight control surfaces were constructed using stiff Kevlar-balsawood sandwich material thereby minimizing the control surface inertia loads and deformations. A typical control surface is shown in figure 5. Miniature hydraulic actuators[4] of the rotating vane type were used both to position the control surfaces statically and to oscillate them at amplitudes of $\pm 6^{\circ}$ over a frequency range from 5 to 15 Hertz. A typical actuator is shown in figure 5.

Instrumentation

The model was instrumented with 242 static pressure orifices and 164 in situ dynamic pressure transducers. Small precision potentiometers were used to measure directly the control surface angular displacement. The model root angle of attack was measured by a digital encoder that was mechanically linked to the turntable in the wind tunnel wall. The wing was mounted to a five-component balance which measured the wing static forces and moments. Six accelerometers were installed in the model to detect wing vibrations. The large amount of instrumentation installed in the model is evident in figure 6.

Wind Tunnel

The Langley Transonic Dynamics Tunnel is a closed-circuit continuous-flow tunnel which has a 4.88-m square test section with slots in all four walls. Mach number and dynamic pressure can be varied simultaneously, or independently, with either air or freon as a test medium. Freon was used for all tests of this investigation.

Data Acquisition and Analysis

General

Acquisition of data from the large number of varied sensors located on this model and analysis of these data in a "near real-time" manner required the use of a computer. The Transonic Dynamics Tunnel facility has a computer uniquely designed and programmed for this purpose.[5] The following paragraphs describe the data acquisition and analysis procedures used during the tests.

Unsteady Pressures Data

Pressure time-history signals from the transducers were digitized and recorded on magnetic tapes for 75-100 cycles of control surface oscillation. During playback of the digital tapes, the Fourier components of the data were determined at the frequency of oscillation of the control surface. Values of pressure coefficient magnitude and phase angle relative to the oscillating control surface position were calculated for each transducer.

Steady Pressure Data

Static pressures were measured using six 48-port scanning valves that were stepped simultaneously from port to port. For each measurement, the pressure was allowed to settle for 0.3 seconds and then was averaged for approximately 1 second to acquire a mean value of pressure coefficient for each orifice.

Force-Balance Data

The lift, drag, and moments were measured using a five-component balance that was mounted between the wing and the side-wall turntable. The data were averaged for approximately 3 seconds to acquire a mean value for each load.

Hinge Moment Data

A technique for measuring static control surface moments was developed using a high quality differential pressure gage installed between the two hydraulic supply lines to the actuator. The mean value of the differential pressure gage output is directly related to the control surface hinge moment. The control surface was oscillated at a low frequency of 0.5 Hertz and amplitude of $\pm 1^{\circ}$ to eliminate the influence of high friction loads in the internal seal of the actuator. The gage signals were averaged for 20 seconds to acquire a mean value for the hinge moment.

Results and Discussion

General

Data from the initial tests included both steady and unsteady pressure measurements, static force-balance measurements, and control surface static hinge-moment measurements. Although steady pressures and force-balance results are not presented herein, the steady

pressure distributions, the drag rise characteristics, and the force and moment coefficients did exhibit characteristics expected of supercritical wing aerodynamics. The following discussions focus on the unsteady pressure results for the design condition: $M = 0.78$, and $\alpha = 2.05^{o}$. The Reynolds number was 2.2×10^{6} based on the average wing chord. Comparisons between measured and calculated results are presented for chordwise distributions of unsteady lifting pressures, spanwise distributions of incremental loads, and static hinge moments.

Measured Unsteady Results

Inboard Control Surface Deflection Results: Chordwise distributions of lifting pressures due to oscillations of the inboard control surface at 10 Hertz are shown in figure 7 for span stations, $\eta = 0.19$ and $\eta = 0.71$. Results are given for oscillatory deflection angles δ of $\pm 2^{o}$, $\pm 4^{o}$, and $\pm 6^{o}$. First, observe the results for $\eta = 0.19$ which is near the mid-span of the inboard control surface. The lifting pressure magnitude increases rapidly from a small value at the leading-edge $x/c = 0$ to a peak near the 80% chord (control surface hinge axis) and then decreases very rapidly to a small value near the trailing-edge $x/c = 1.0$. The corresponding phase angle results show a large phase lag near the leading-edge that decreases to zero near the 65% chord and shows a phase lead over the rear portion of the chord. The magnitude of ΔC_p increases with control surface deflection amplitude in an approximate linear manner over the entire chord. That is, the magnitude of ΔC_p for $\delta = \pm 6^{o}$ is about three times the value for $\delta = \pm 2^{o}$. The phase angle results are essentially independent of the amplitude of control surface deflection. Second, observe the results for $\eta = 0.71$ which is near the mid-span of the outboard control surface. Although the oscillating control surface is well removed from the pressure measurement station, its effect on the unsteady pressures is significant. The magnitude rises sharply to a peak near the 25% chord, drops abruptly to near zero at the 40% chord and remains near zero to the trailing-edge. Except for the wide excursions in phase angle near the 40% chord, the phase angle trends for the outboard station are similar to those at the inboard station in that a large phase lag exists at the leading-edge and decreases toward zero going rearward along the chord.

Inboard Control Surface Frequency Results:

The chordwise distributions of lifting pressures for three frequencies of the inboard control surface oscillating at amplitude of $\pm 6^{o}$ are presented in figure 8 for $\eta = 0.19$ and $\eta = 0.71$. Results are shown for frequencies of 5, 10, and 15 Hertz which correspond to reduced frequency values k of about 0.1, 0.2, and 0.3. For $\eta = 0.19$, control surface frequency has a much greater effect on phase angles than on magnitudes of unsteady pressures. The largest effects occur at the leading-edge where the 5 Hertz data show a phase lag of about 40^{o} and the 15 Hertz data show a phase lag of about 120^{o}. For $\eta = 0.71$, the results indicate the effects of frequency to be much more pronounced in the phase angle data than in the magnitude data. These results show again the significant influence the inboard oscillating control surface has on unsteady lifting pressures far outboard on the wing.

Outboard Control Surface Deflection and Frequency Results: Unsteady lifting pressure distribution results for the oscillating outboard control surface are presented in figures 9 and 10. The deflection and frequency effects show general trends similar to those discussed for the oscillating inboard control surface. A significant difference, however, is the sharp hump in the lifting pressure magnitude data near the 50% chord. Although data for $\eta = 0.19$ are not presented in the figures, neither the magnitude nor phase angle data at this station was affected by the oscillating outboard control surface.

Comparison of Measured and Calculated Results

General: The calculated results presented herein were obtained from an analysis based on linear theory for the acceleration potential on zero thickness lifting surfaces.[3] This subsonic kernel-function method accounts for edge and hinge line singularities of the control surface. Effects of airfoil thickness are partially accounted for by modifying the local streamwise velocity.

Chordwise Lifting Pressure: A comparison between measured and calculated chordwise distribution of lifting pressures at $\eta = 0.19$ generated by oscillating the inboard control surface is presented in figure 11. These results are for $M = 0.78$ and control surface frequency of 10 Hertz. The variation of lifting pressure magnitude per degree and of phase angle, referenced to the control surface position, is plotted as a function of fraction of chord. Measured and calculated magnitude results show reasonable agreement up to the 20% chord. From 20% to 70% chord, the calculations underestimate the measured data which are characterized by a broad hump that peaks near the 50% chord. Calculations overestimate measured data behind the hinge axis at 80% chord. The calculated results show a smaller phase lag than the measured data ahead of the 40% chord. Aft of the 40% chord, the calculated and measured results are in good agreement.

Spanwise Incremental Loads: An additional comparison between calculated and measured results is presented in figure 12 as spanwise incremental loads generated by a deflected inboard control surface. Figure 12 shows both steady and unsteady results as percent increase in lifting load (magnitude), above that of the basic wing load with no deflected control surface, plotted as a function of fraction of semispan. Measured steady data for the control deflected statically $+6^{o}$ are represented by circle symbols. The measured unsteady data for the control surface oscillating $\pm 6^{o}$ at 10 Hertz are represented by square symbols. Corresponding calculated steady results are shown as the solid line, and unsteady results are shown as the dashed line. Comparisons of the steady and unsteady magnitude

results, measured and calculated, show no significant differences. The magnitude of wing incremental loading, therefore, must be primarily a function of the control surface deflection angle and does not depend on whether the control surface is deflected statically or dynamically at this frequency. Phase effects are not included in the unsteady magnitude results. Comparison between measured and calculated magnitudes, however, indicates a significant difference for both the steady and unsteady cases. Across the entire span, the calculated incremental loads are lower than the measured loads.

The poor agreement between measured and calculated results is probably due to the fact that the present analysis does not account for transonic, nonlinear, or viscous effects.

Static Hinge Moment: Measured hinge moments for the inboard trailing-edge control surface at Reynolds numbers of 2.2×10^6 and 4.7×10^6 are presented in figure 13. The results are shown in terms of hinge-moment coefficient per degree as a function of Mach number. Also shown in figure 13 is a comparison between the measured and calculated static hinge moment results. These results show reasonably good agreement over the Mach number range from 0.4 to 0.8.

Concluding Remarks

An experimental investigation has been conducted on an aspect ratio 10.8 supercritical wing model with oscillating control surfaces. Selected measured unsteady results from the initial wind-tunnel tests have been presented and discussed. Briefly, the measured results show that unsteady lifting pressures generated by oscillating control surfaces are substantial. In particular, the inboard oscillating control surface was shown to have a significant influence on the unsteady lifting pressures far outboard on the wing. Also, measured data were compared with calculated results obtained using a subsonic lifting surface theory. Results indicate a need for better prediction methods in the transonic speed range.

In summary, the purpose of this model research program is to produce a comprehensive data base of measured transonic unsteady pressure for use in designing active control systems and for use in validating transonic unsteady aerodynamic theories currently being formulated.

References

[1]Tijdeman, Hendrik, "Investigation of the Transonic Flow Around Oscillating Airfoils," NLR TR-77090-U, 1977.

[2]Borland, C. J., "A Bibliography of Recent Developments in Unsteady Transonic Flow," Vol. 1, AFFDL-TR-78-189, Feb. 1979.

[3]Rowe, W. S., Sebastian, J. D., and Petrarca, J. R., "Reduction of Computer Usage Costs in Predicting Unsteady Aerodynamic Loadings Caused by Control Surface Motions--Analysis and Results," NASA CR-3009, March 1979.

[4]Bergmann, Gerald E., and Sevart, Francis D., "Design and Evaluation of Miniature Control Surface Actuation Systems for Aeroelastic Models," J. Aircraft, Vol. 12, No. 3, March 1975, pp. 129-134.

[5]Cole, Patricia H., "Wind Tunnel Real-Time Data Acquisition System," NASA TM-80081, April 1979.

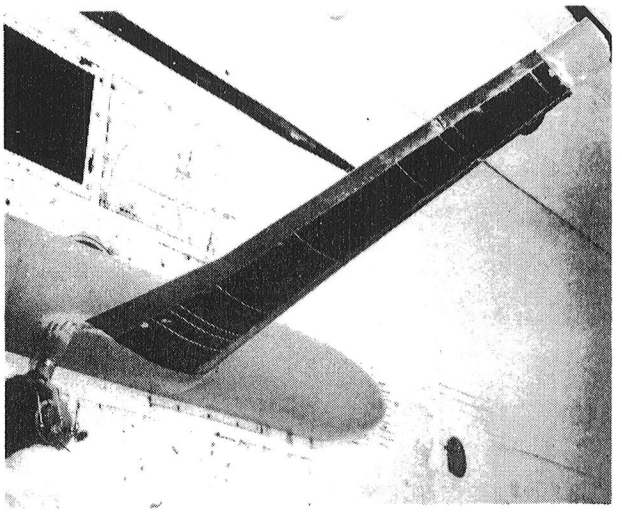

Fig. 1.- Photograph of complete model mounted in wind tunnel.

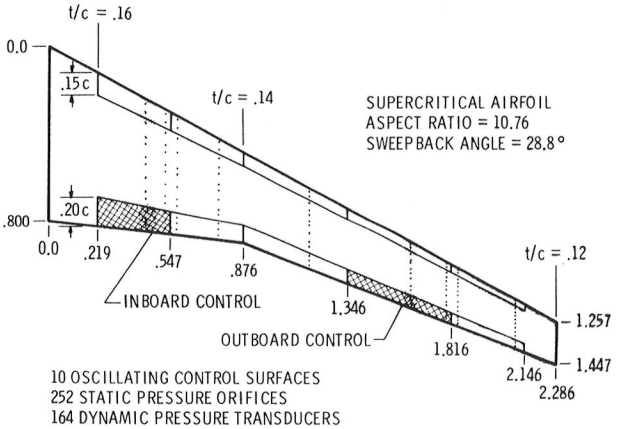

Fig. 2.- Sketch of wing planform (all linear dimensions are in meters).

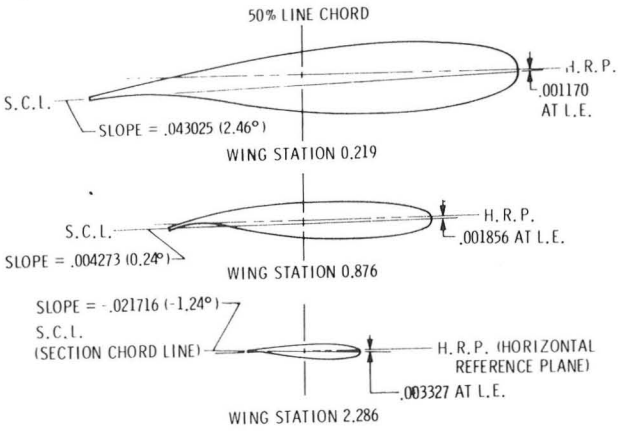

Fig. 3.- Pictorial view of supercritical airfoil shape at three wing stations.

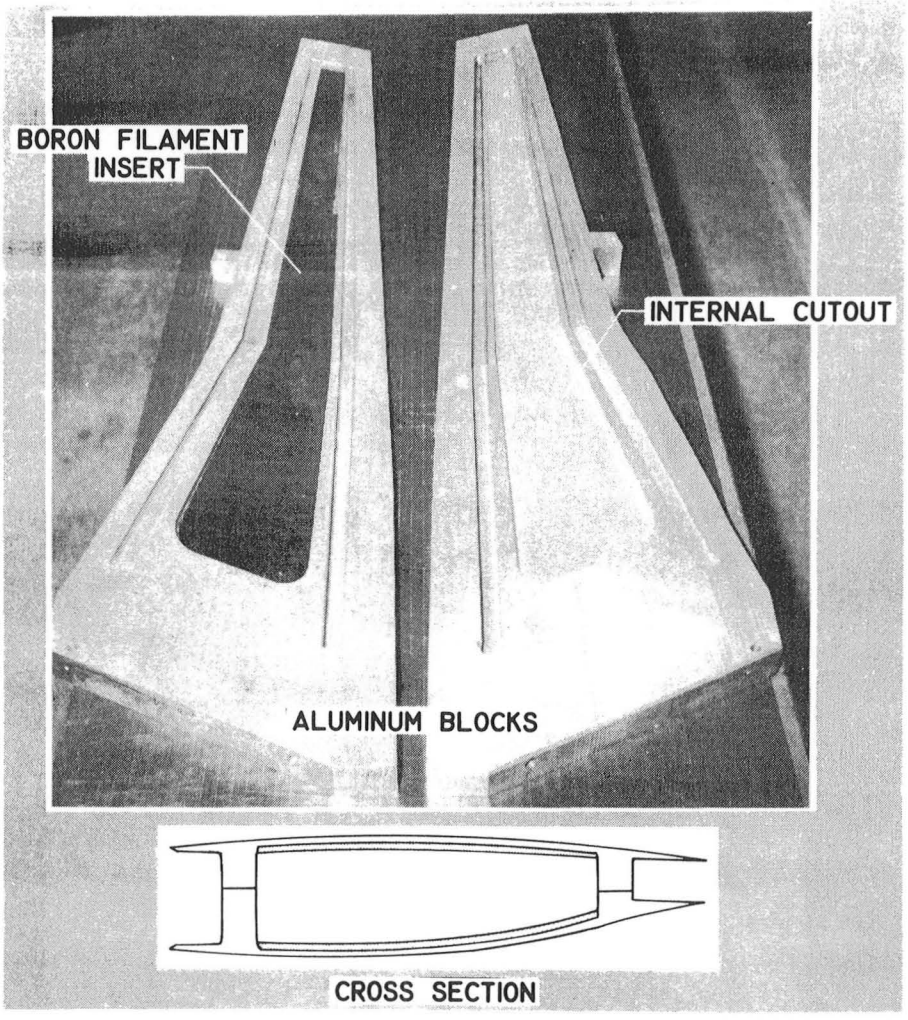

Fig. 4.- Illustration of wing box construction.

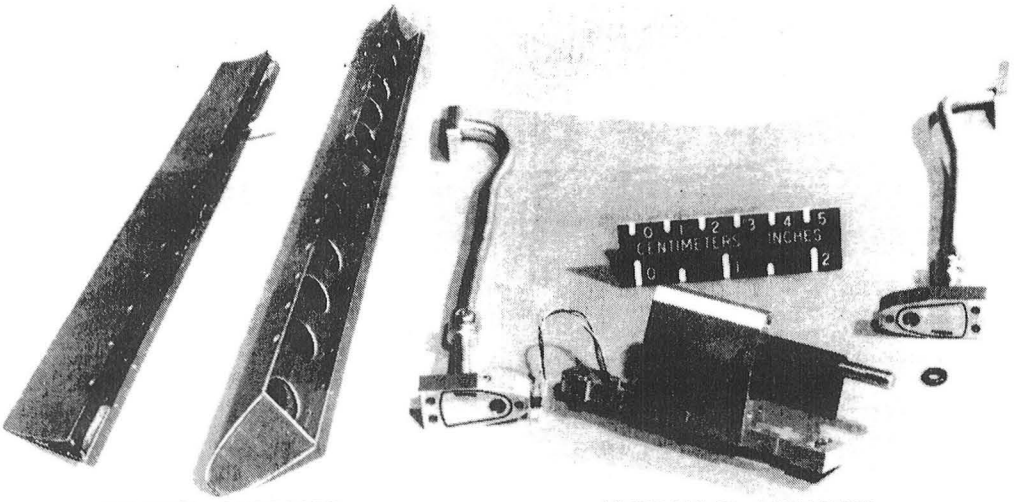

Fig. 5.- Photograph of typical control surface and hydraulic actuator.

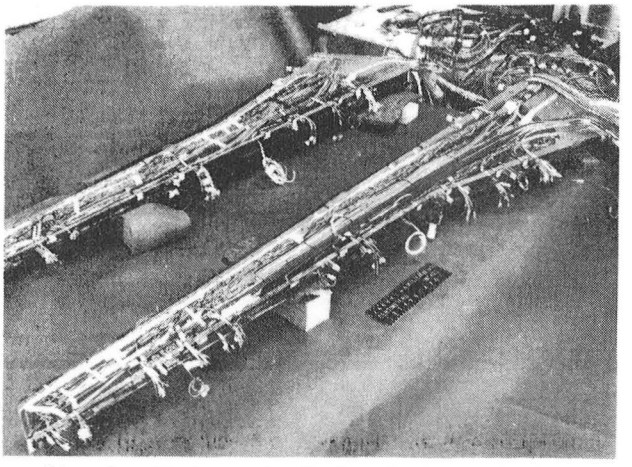

Fig. 6.- Photograph of wing instrumentation.

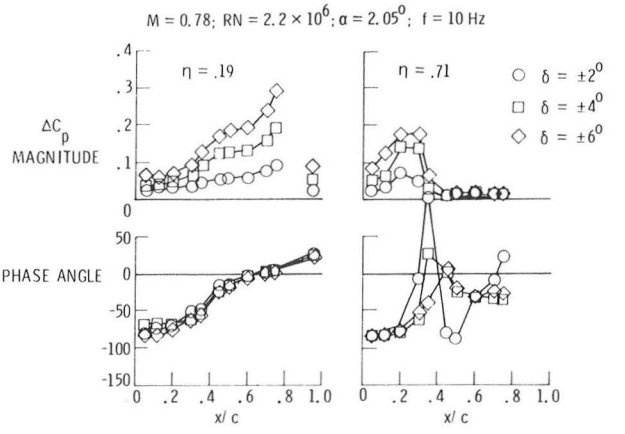

Fig. 7.- Inboard control surface oscillating deflection results.

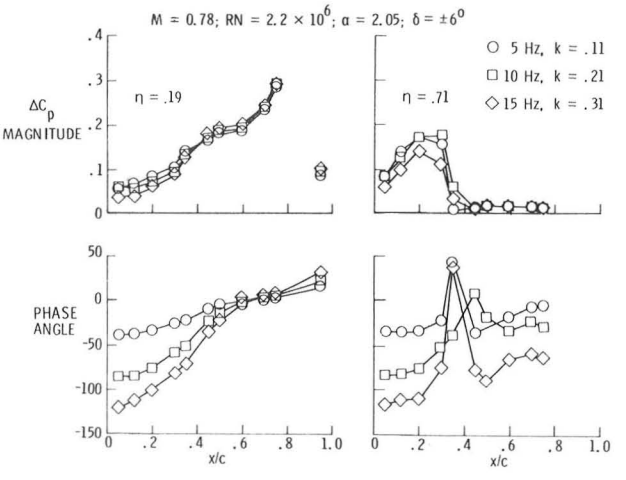

Fig. 8.- Inboard control surface oscillating frequency results.

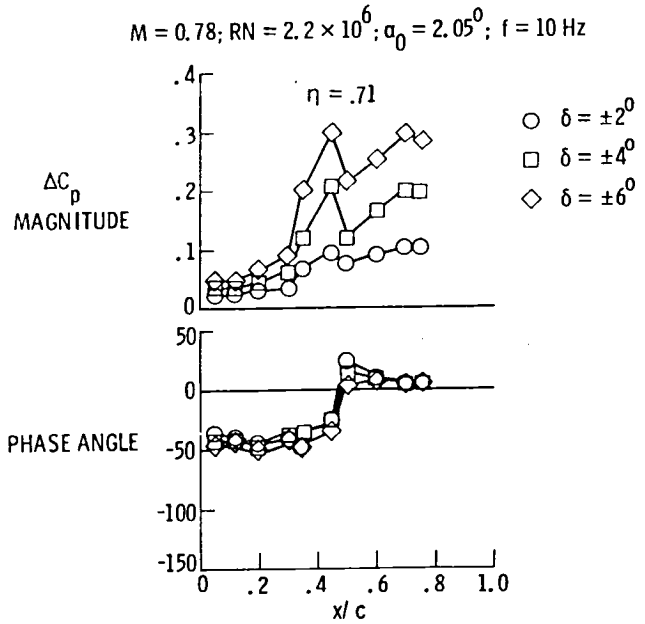

Fig. 9.- Outboard control surface oscillating deflection results.

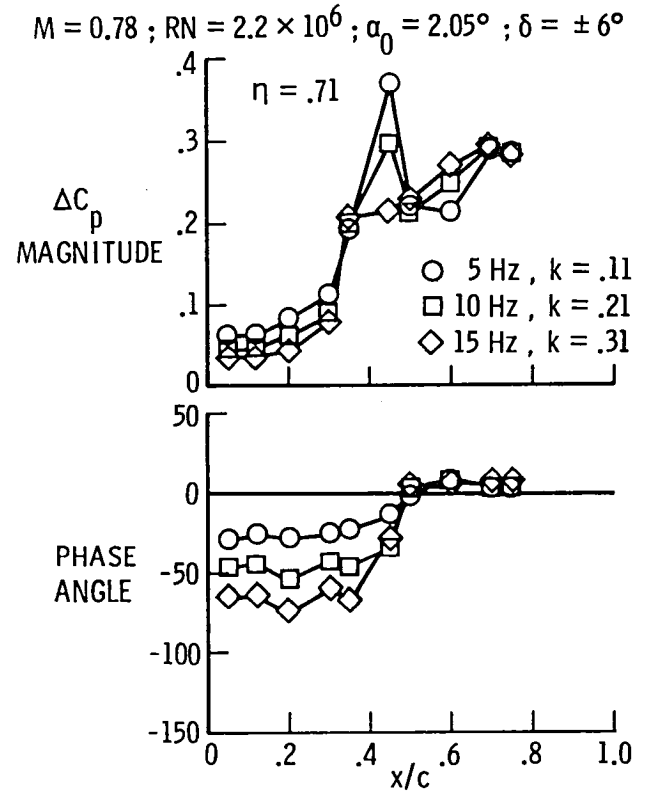

Fig. 10.- Outboard control surface oscillating frequency results.

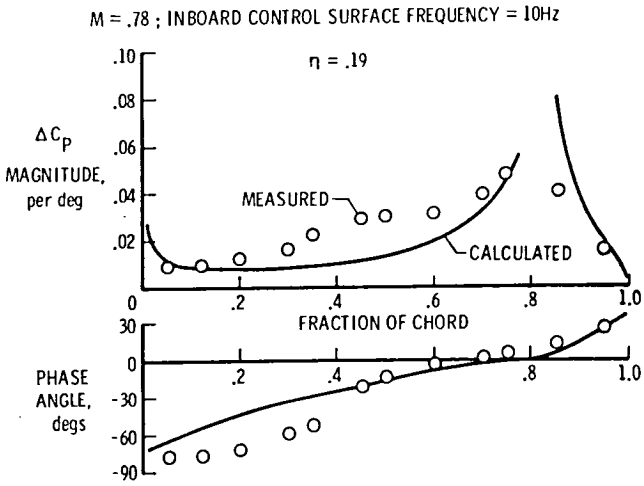

Fig. 11.- Comparison of measured and calculated chordwise unsteady lifting pressure distributions.

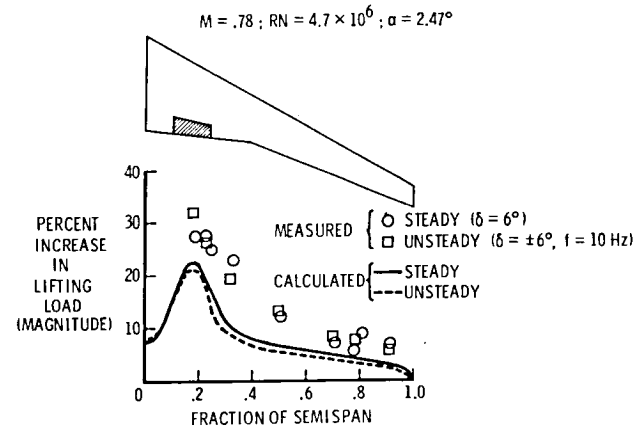

Fig. 12.- Comparison of measured and calculated spanwise incremental lifting loads generated by a deflected control surface.

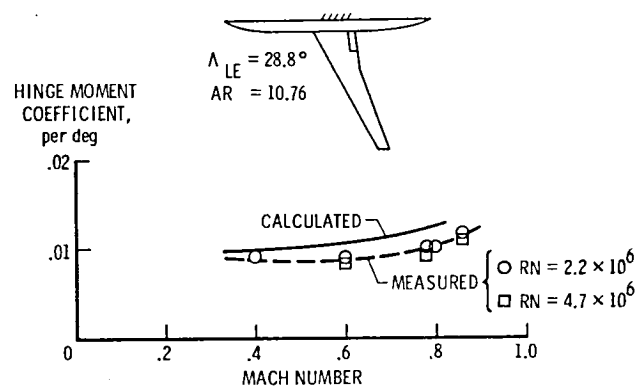

Fig. 13.- Comparison of measured and calculated static hinge moments.

1. Report No.	2. Government Accession No.	3. Recipient's Catalog No.
NASA TM-81788		

4. Title and Subtitle	5. Report Date
Transonic Unsteady Airloads on an Energy Efficient Transport Wing with Oscillating Control Surfaces	March 1980
	6. Performing Organization Code

7. Author(s)	8. Performing Organization Report No.
M. C. Sandford, R. H. Ricketts, F. W. Cazier, Jr., and H. J. Cunningham	
	10. Work Unit No. 534-02-13-21

9. Performing Organization Name and Address	11. Contract or Grant No.
NASA Langley Research Center Hampton, Virginia 23665	
	13. Type of Report and Period Covered Technical Memorandum

12. Sponsoring Agency Name and Address	14. Sponsoring Agency Code
National Aeronautics and Space Administration Washington, DC 20546	

15. Supplementary Notes

Technical Paper Presented at the AIAA/ASME/ASCE/AHS 21st Structures, Structural Dynamics, and Materials Conference, Seattle, Washington, May 12-14, 1980

16. Abstract

An aspect-ratio 10.8 supercritical wing with oscillating control surfaces is described. The wing is instrumented with 252 static orifices and 164 in situ dynamic pressure transducers for studying the effects of control surface deflection on steady and unsteady pressures at transonic speeds. Selected results from initial wind-tunnel tests conducted in the Langley Transonic Dynamics Tunnel are discussed. Unsteady pressure results are presented for two trailing-edge control surfaces oscillating separately at the design Mach number of 0.78. Some experimental results are compared with analytical results obtained by using linear lifting-surface theory.

17. Key Words (Suggested by Author(s))	18. Distribution Statement
Unsteady aerodynamics Transonic speed Control surfaces Supercritical wing	Unclassified - Unlimited Subject Category 02

19. Security Classif. (of this report)	20. Security Classif. (of this page)	21. No. of Pages	22. Price*
Unclassified	Unclassified	7	$4.00

For sale by the National Technical Information Service, Springfield, Virginia 22161